Journal of
Composites Science

MDPI

Review

Materials Development Using High-Energy Ball Milling: A Review Dedicated to the Memory of M.A. Korchagin

Dina V. Dudina [1,2,*] and Boris B. Bokhonov [1]

[1] Institute of Solid State Chemistry and Mechanochemistry SB RAS, Kutateladze str. 18, 630128 Novosibirsk, Russia; bokhonov@solid.nsc.ru
[2] Lavrentyev Institute of Hydrodynamics SB RAS, Lavrentyev Ave. 15, 630090 Novosibirsk, Russia
* Correspondence: dina1807@gmail.com

Abstract: High-energy ball milling (HEBM) of powders is a complex process involving mixing, morphology changes, generation and evolution of defects of the crystalline lattice, and formation of new phases. This review is dedicated to the memory of our colleague, Prof. Michail A. Korchagin (1946–2021), and aims to highlight his works on the synthesis of materials by self-propagating high-temperature synthesis (SHS) and thermal explosion (TE) in HEBM mixtures as important contributions to the development of powder technology. We review results obtained by our group, including those obtained in collaboration with other researchers. We show the applicability of the HEBM mixtures for the synthesis of powder products and the fabrication of bulk materials and coatings. HEBM influences the parameters of synthesis as well as the structure, phase composition, phase distribution (in composites), and grain size of the products. The microstructural features of the products of synthesis conducted using the HEBM precursors are dramatically different from those of the products formed from non-milled mixtures. HEBM powders are also suitable as feedstock materials for depositing coatings by thermal spraying. The emerging applications of HEBM powders and future research directions in this area are discussed.

Keywords: high-energy ball milling; powder; microstructure; composites; self-propagating high-temperature synthesis; thermal explosion; sintering; coatings

Citation: Dudina, D.V.; Bokhonov, B.B. Materials Development Using High-Energy Ball Milling: A Review Dedicated to the Memory of M.A. Korchagin. *J. Compos. Sci.* **2022**, *6*, 188. https://doi.org/10.3390/jcs6070188

Academic Editor: Francesco Tornabene

Received: 17 June 2022
Accepted: 23 June 2022
Published: 25 June 2022

1. Introduction

High-energy ball milling (HEBM) is a treatment of powders, which uses the action of the milling media to mix, disperse, activate and form composite structures [1–4]. The milling devices exist in various designs. Usually, they are divided into two groups: low-energy and high-energy mills [5]. The processes occurring during HEBM are deformation, defect accumulation, fracture, welding, structural refinement, and breakage/formation of chemical bonds. During HEBM, composite agglomerates form, which are also referred to as mechanocomposites [6,7]. Those are particles that contain all components of the starting powder mixture. They may also contain the reaction products owing to a partial interaction, the reaction yield depending on the milling time and milling energy. The internal structure of mechanocomposites determines their reactivity and consolidation behavior. The non-equilibrium structure of the material can be preserved in the bulk state if proper methods of consolidation are applied.

Several reviews dealing with mechanical milling have been published, focusing on different aspects of the process or its applications. Suryanarayana & Nasser Al-Aqeeli [8] presented a systematic review of nanocomposites produced by mechanical milling. They considered the possibility of introducing a high volume fraction of reinforcing particles in the matrices as one of the advantages of mechanical milling in the processing of composite materials. The synthesis of intermetallics by HEBM was reviewed by Hadef [9]. Rogachev [10] presented the state of the art in the synthesis via exothermic reactions in

the mechanically activated mixtures and discussed the role of structural transformations occurring during milling in the increase in the reactivity of the components of the mixture. Zhang [1] presented an overview of the use of HEBM for the production of powders of different chemical nature and composition, including amorphous and nanocrystallitne powders. The irregular shape of the particles and a high level of strain hardening of HEBM products were considered the key factors influencing the sintering behavior of the powders.

The present article deals with the materials development aspects of HEBM, namely, the phase composition and structural features of the products obtained from the ball-milled precursors. This review is dedicated to the memory of our colleague, Prof. Michail A. Korchagin (1946–2021). He conducted his research at the Institute of Solid State Chemistry and Mechanochemistry SB RAS. His works on the synthesis of materials by self-propagating high-temperature synthesis (SHS) and thermal explosion (TE) in HEBM mixtures are important contributions to the development of powder technology.

We review results obtained by our group, including those obtained in collaboration with other research laboratories. First, the features of thermally induced chemical reactions in HEBM powders are discussed. Examples of reactions occurring in the SHS/TE mode and slow reactions occurring upon annealing of the powders are elaborated. Second, examples of materials obtained by consolidation of HEBM powders are considered. Third, the possibilities of using HEBM powders for depositing coatings are described. We show that the use of HEBM precursors allows producing powder products of particular morphologies and bulk materials with tailorable microstructural characteristics.

In general, planetary ball mills are widely used in industry and laboratory practice [11]. In the examples discussed in Section 2 of this review, for conducting HEBM, planetary ball mills of AGO-2 model [12] were used. This model was developed at the Institute of Solid State Chemistry and Mechanochemistry SB RAS. The AGO-2 mills are of friction type and have two vials, which are water-cooled. A general view and schematic of an AGO-2 mill are shown in Figure 1. The vial rotation frequency in the AGO-2 mills working in different modes can be found in ref. [13].

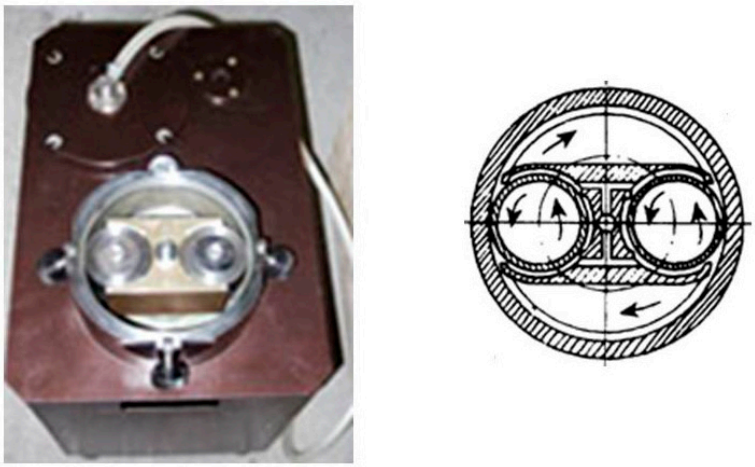

(**a**) (**b**)

Figure 1. (**a**) A general view of an AGO-2 mill without a lid: two vials and a planetary carrier are rotating inside the casing. (**b**) A schematic (top view) of an AGO-2 mill: the vials are in planetary motion.

2. Materials Development Using High-Energy Ball-Milled (HEBM) Precursors

2.1. Thermally Induced Chemical Reactions in HEBM Powders and Synthesis of Powder Products

2.1.1. Self-Propagating High-Temperature Synthesis (SHS) from HEBM Powder Precursors

Combustion reactions conducted under controlled conditions can be used for the synthesis and microstructure tailoring of a wide range of materials [10,14–16]. The formation of nano-grained intermetallics is possible by SHS in reaction mixtures subjected to HEBM [17,18]. It was found that a transition from the mode of interaction involving a liquid

phase to the solid-state combustion mode occurs when HEBM is applied to the reaction mixtures [17]. The possibility of SHS reactions in the solid-state mode was attributed to the formation of mechanocomposites, in which the initial reactants are mixed and dispersed at the nano-level. Furthermore, the reactants have a well-developed interface with each other and a highly defect crystalline structure. The products of SHS conducted in a 3Ni+Al mixture subjected to preliminary HEBM for 30 s consisted of Ni, Ni_3Al, and NiAl. As the milling time was increased, the concentrations of Ni and NiAl in the SHS products decreased. After 2.5 min of HEBM, the SHS product was single-phase Ni_3Al.

The milling intensity was found to influence the phase evolution of the SHS-products in the 3Ni+Al mixture with the milling time [18]. An important effect operating during SHS of HEBM mixtures is reverse quenching. Defects produced by HEBM are not annealed in the heating zone and are preserved in the sample until the beginning of the chemical interaction in the leading zone of the SHS wave. Annealing of defects in the leading zone increases the reactivity of the components.

It should be noted that the mechanical properties of the material of the particles change with the milling time. The phase and structural transformations occurring during HEBM of a 3Ni+Al mixture were studied in a separate investigation [19]. It was shown that, under HEBM conditions, a solid solution of aluminum in nickel Ni(Al), Ni_3Al and NiAl form within several minutes of treatment. The synthesis of hard phases and structural refinement provided a gradual increase in the microhardness of the particles (measured on the mounted and polished cross-sections of the particles). The microhardness of the particles of the powder ball-milled for 10.5 min was 8.34 GPa.

Combustion reactions in ternary metallic systems result in the formation of complex alloy products. Alloys with a quasicrystalline structure were obtained by a combination of HEBM and SHS [20,21]. The stable decagonal $Al_{72}Ni_{20}Co_8$ and $Al_{72}Ni_{12}Co_{16}$ quasicrystals were obtained by SHS in HEBM mixtures of the metals [20]. It was impossible to ignite a SHS reaction in the non-milled mixtures of the metals. It was noted that short HEBM is an alternative to the use of a "chemical furnace" to facilitate ignition. A possibility of using SHS for the formation of quasicrystals was also demonstrated for another composition, $Al_{63}Cu_{25}Fe_{12}$ [21]. Figure 2 shows the X-ray diffraction patterns of the products of SHS in the mixtures milled for 30–90 s. It is seen that 30 s of milling was sufficient to form a product with an icosahedral phase as the main phase.

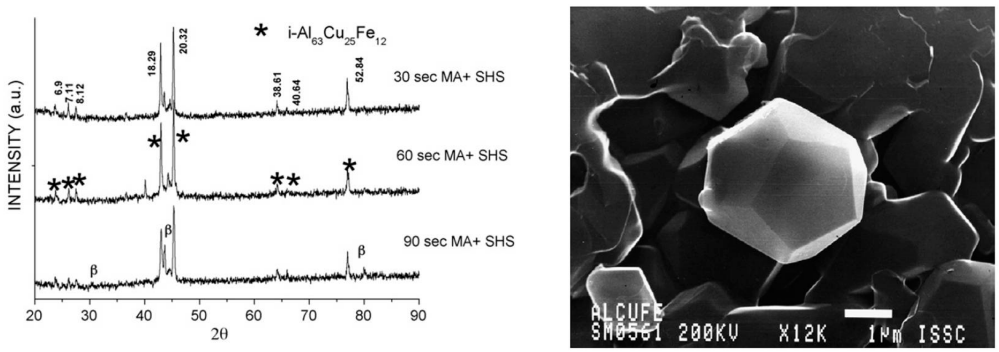

(**a**) (**b**)

Figure 2. X-ray diffraction (XRD) patterns of the products of self-propagating high-temperature synthesis in a Al-Cu-Fe powder mixture, indicating the formation of $Al_{63}Cu_{25}Fe_{12}$ quasicrystals, the time of HEBM (or mechanical activation, abbreviated as MA in the image) was 30, 60 or 90 s (**a**). Morphology of the synthesized quasicrystals, secondary electron (SE) image (**b**). Reprinted from [21], Copyright (2007), with permission from Elsevier.

SHS in HEBM mixtures was successfully used for the fabrication of MAX phases, Ti_3SiC_2 and Ti_3AlC_2 [22]. Single-phase Ti_3SiC_2 was obtained using the following approach: two mixtures were prepared with the overall composition corresponding to the nominal

composition of the compound. Those mixtures were HEBM for different durations. After that, the HEBM mixtures were blended to make a precursor powder for the subsequent SHS.

Composite materials can be synthesized by SHS using compounds as reactants [23–25]. It was shown that HEBM mixtures of TiNi and carbon can be ignited so that the interaction occurs in the TE mode [23]. SHS was realized in a HEBM mixture of the 3Ti+2BN composition. The products consisted of grains 10–30 nm in size [24]. Those grains were surrounded by even finer particles. It was confirmed that the coarser grains are those of TiB_2, while the finer ones are TiN. Such small grains were a result of combustion occurring in the solid-state mode. It was emphasized that the possibility of SHS depends much on the capability of the powders to form mechanocomposites upon HEBM, and not so much on the grain size of the reactants. On the plots of the combustion temperature and combustion rate versus the time of HEBM, there was a region, within which the combustion could not be initiated. The effect was attributed to the specific structural features of the particles formed in the milled mixture.

HEBM ternary mixtures can serve as precursors of metal-ceramic composites when the interaction between the two reactants results in the formation of particles distributed in a matrix (the third component of the mixture) [26–28]. Figure 3 shows transmission electron microscopy (TEM) images of the Ti-B-Cu mixture subjected to HEBM and the product of SHS (TiB_2-Cu), which was additionally milled to reduce its particle size. Both powders are nanostructured. The TiB_2-Cu powders were used to produce bulk nanocomposite materials by shock wave consolidation [29] and spark plasma sintering (SPS) [26,27,30].

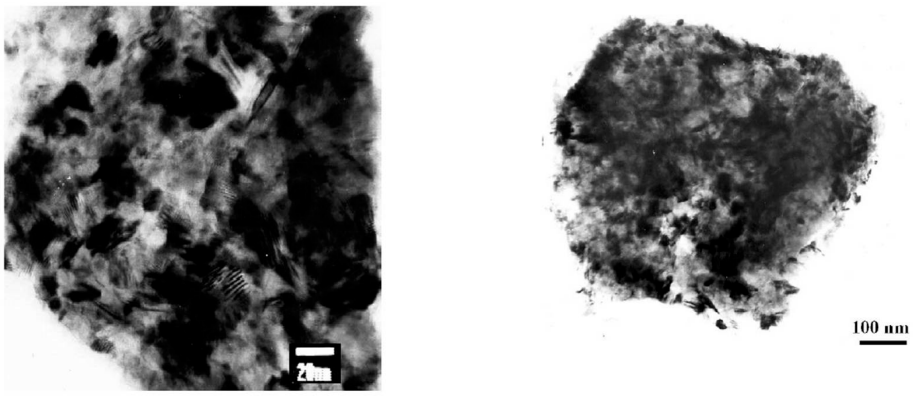

(**a**) (**b**)

Figure 3. (**a**) Transmission electron microscopy (TEM) image of the Ti–B–Cu powder, HEBM for 2 min, (**b**) TEM image of the Cu–57 vol.% TiB_2 composite powder (the product of SHS reaction was HEBM for 5 min). Reprinted from [26], Copyright (2006), with permission from Elsevier.

2.1.2. Synthesis in the Thermal Explosion (TE) Mode from HEBM Powder Precursors

When the synthesis occurs in TE mode, the reaction is initiated in the system over its entire volume. A series of studies have been conducted to analyze the effect of HEBM on the parameters of TE of mixtures of different compositions [31–39]. It was shown that the duration of HEBM of the reaction mixtures influences the ignition temperature T_{ign} and the maximum temperature T_{max} of TE.

It is interesting to trace the evolution of the structure of the composite agglomerates during HEBM and find correlations between the structural changes and changes in the characteristic temperatures of TE. In the mechanically milled Ti-C-3Cu mixtures, it was possible to conduct the synthesis of TiC-Cu composites in the TE mode [38,39]. Figure 4 shows the microstructure evolution of the Ti-C (carbon black)-3Cu powder agglomerates with the milling time. In the structure of composite particles formed after 3 min of milling, gray islands (stripes) can be distinguished. They were proved to be the titanium phase. After 10 min of milling, the microstructure of the agglomerates becomes more uniform, and the titanium islands disappear. In Figure 5, the thermograms of TE of the mixtures

milled for 3–10 min are presented. The characteristic temperatures, T_{ign} and T_{max}, decrease with the milling time [38]. A decrease in T_{ign} is due to the development of the interface between the reactants and accumulation of defects in their crystalline structure. T_{max} decreases with the milling time owing to partial transformation of the reactants during HEBM. For the mixture milled for 10 min, T_{max} is lower than the melting point of copper. The products of TE in all mixtures are two-phase TiC-Cu composites. The microstructure of the product of TE of the mixture milled for 10 min is shown in Figure 6. No evidence of melting-induced phase redistribution (formation of TiC-depleted areas) was found, which agrees with the measured value of T_{max}. As shown in Section 2.2, this is an important observation, which helps rationalize the structure formation of the composite during electric current-assisted sintering.

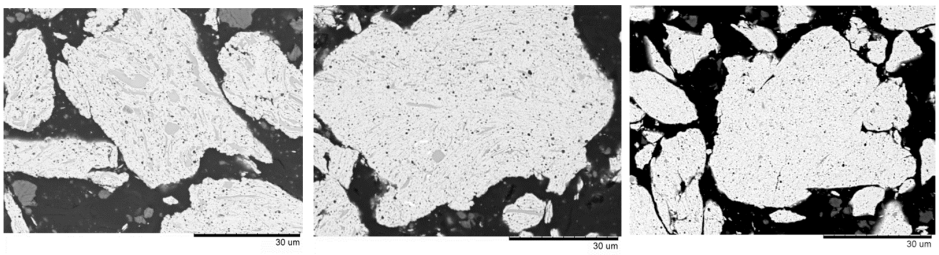

(**a**) (**b**) (**c**)

Figure 4. Microstructure (back-scattered electron (BSE) images) of Ti-C (carbon black)-3Cu powder agglomerates of the HEBM mixtures: milling time 3 min (**a**), 5 min (**b**) and 10 min (**c**). Reprinted from [39], Copyright (2021), with permission from Elsevier.

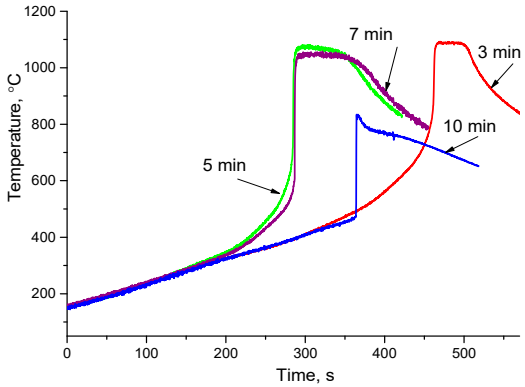

Figure 5. Thermograms of thermal explosion (TE) in HEBM Ti-C (carbon black)-3Cu mixtures. Milling time is given next to the curves. Reprinted from [38], Copyright (2021), with permission from Elsevier.

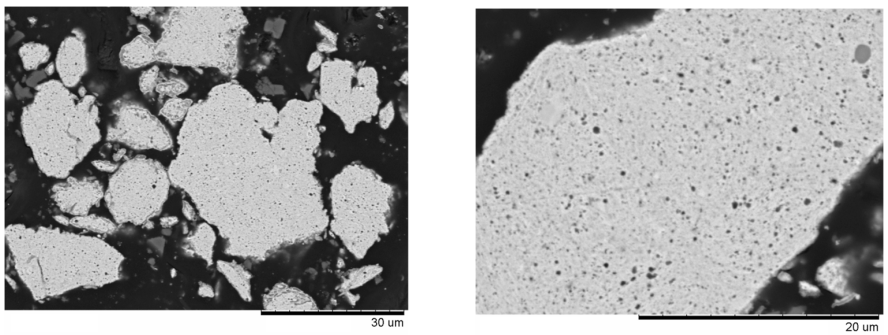

(**a**) (**b**)

Figure 6. Microstructure (BSE images) of the composite particles of Ti-C-3Cu after TE (**a**), 10 min of HEBM (**b**), different magnifications. Reprinted from [38], Copyright (2021), with permission from Elsevier.

The influence of the duration of HEBM of a 3Ti+Al powder mixture on the phase composition of the TE products and the parameters of TE was studied in ref. [34]. TEM studies showed that the size of metallic particles in the mixture HEBM for 6 min is below 100 nm. The thermograms of TE of mixtures milled for (60 J g^{-1}), 3 min (180 J g^{-1}), 5 min (300 J g^{-1}) and 7 min (420 J g^{-1}) obtained at a heating rate of 50 K min^{-1} are shown in Figure 7. The input energy given above is used to plot the graphs in Figure 8. The time to reach the maximum temperature was taken as the reaction time. It is seen that the composition of the products of TE, the reaction time and T_{max} depend on the milling duration. It was suggested that the concentrations of defects in the crystalline structures and internal stress gradients increase with the milling time causing the observed differences in the behavior of the mixtures upon TE.

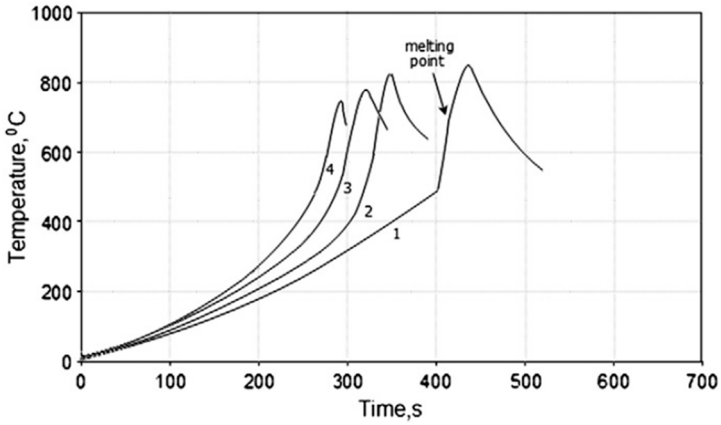

Figure 7. Thermograms of thermal explosion (TE) of a HEBM 3Ti+Al mixture. 1—1 min; 2—3 min; 3—5 min; 4—7 min of HEBM. Reprinted from [34], Copyright (2012), with permission from Elsevier.

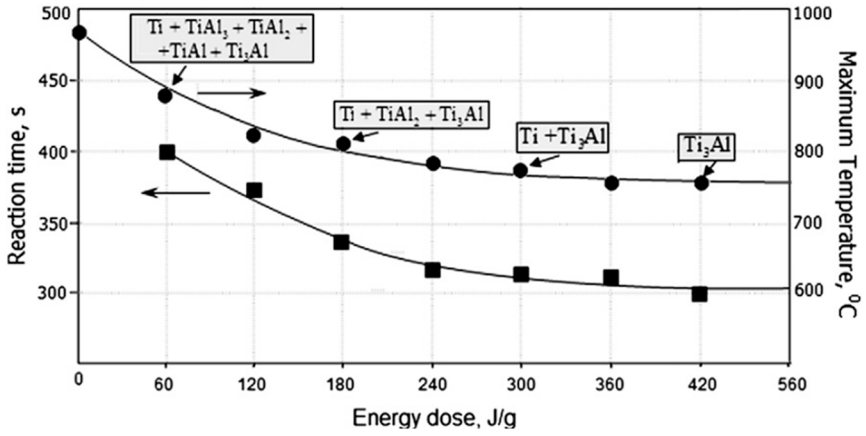

Figure 8. The dependence of the reaction time and T_{max} on the energy dose. The composition of the products of TE is given. Reprinted from [34], Copyright (2012), with permission from Elsevier.

As a synthesis method, TE in HEBM mixtures produces excellent results, as the forming products possess fine grain sizes. For example, TE in a HEBM W+C mixture allowed obtaining a single-phase carbide WC with sub-micrometer grains [33]. The synthesized WC was a powder consisting of particles 1–20 μm in size; the size of WC grains was 0.2–0.5 μm.

2.1.3. Synthesis of Materials by Annealing of HEBM Powder Precursors

HEBM powders were used as precursors in the synthesis of core-shell particles, namely, particles encapsulated in a graphite shell [40–42] or hexagonal boron nitride, BN, shell [43]. The core-shell structures formed upon annealing of the HEBM powders. Particles with graphitic shells and metallic [40] or carbide [41,42] cores were synthesized. Annealing of mixtures of amorphous carbon (soot) with iron or nickel HEBM for 1–2 min results in the

formation of onion-like structures [40]. If the mixture is HEBM for more than 5 min, carbon-encapsulated metal particles form upon annealing. During HEBM of Mo-amorphous carbon mixtures, nano-sized particles of Mo_2C formed (Figure 9) [41]. Annealing of HEBM mixtures at 830 °C resulted in the formation of encapsulated particles of molybdenum carbide Mo_2C (Figure 10). A mechanism of the formation of polyaromatic carbon-encapsulated carbide or metal particles was proposed. During HEBM, a metastable metal-carbon compound forms. Upon annealing, it decomposes into the metal or carbide phase and polyaromatic carbon precipitating as layers on the metal/carbide surface and forming a shell.

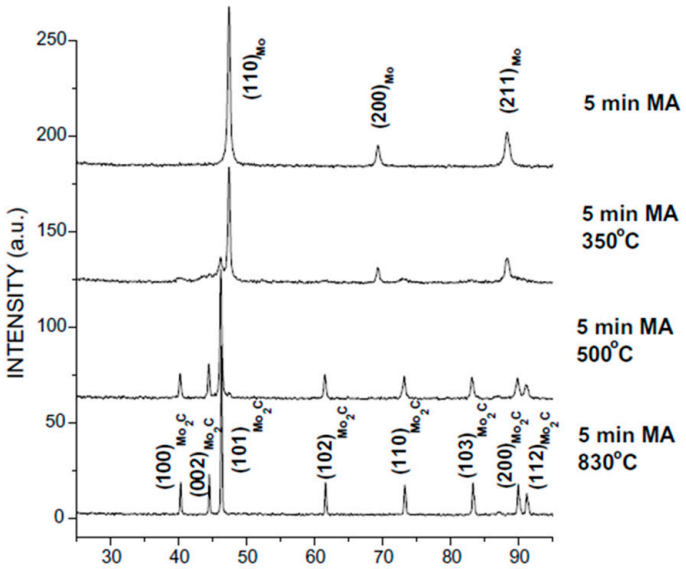

Figure 9. XRD patterns (Co Kα irradiation) of molybdenum–amorphous carbon mixtures after HEBM for 5 min and annealing at 350, 500 and 830 °C. Reprinted from [41], Copyright (2004), with permission from Elsevier.

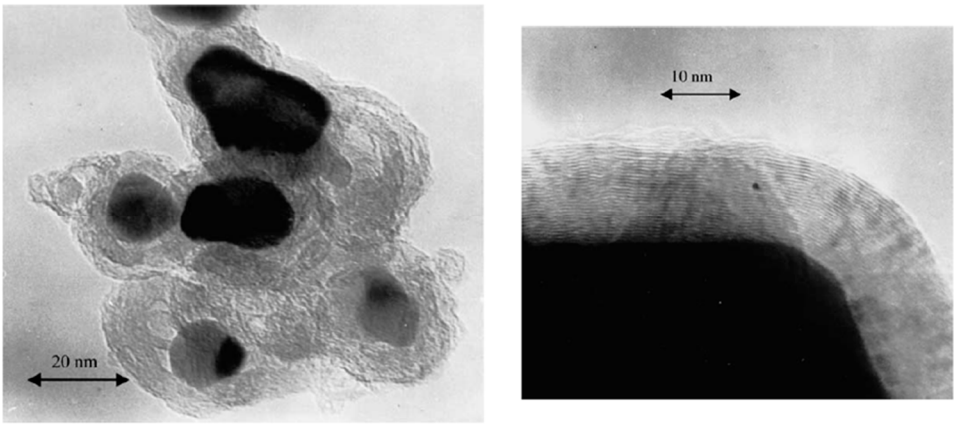

(**a**) (**b**)

Figure 10. (**a**) TEM image of the encapsulated molybdenum carbide, Mo_2C, particles formed during annealing of a HEBM molybdenum–amorphous carbon 1.5Mo-C mixture. (**b**) HREM image of the surface of molybdenum carbide, Mo_2C, particles encapsulated by polyaromatic carbon formed during annealing of the HEBM 1.5Mo-C mixture. Reprinted from [41], Copyright (2004), with permission from Elsevier.

2.2. Consolidation of HEBM Powders

HEBM powders should be consolidated by non-equilibrium methods in order to preserve their fine-grained structure. Reactive sintering of HEBM needs to be conducted

under conditions that allow using the potential of the reaction mixtures to form the fine-grained products [44]. In general, the HEBM systems are interesting objects for studying the sintering/consolidation processes, as the highly defect states and their fine-grained structure will influence the densification mechanisms and kinetics. Multiple opportunities for the materials development lie in the combination of mechanical milling and SPS [45–50].

In our studies, we have shown that the SPS behavior of the powder depends on the morphology of the particles [51]. As long as the shape of the particles does not change significantly upon the application of pressure, the contact area between the spherical particles remains small. Particles of platelet shape contact each other over a large area. When sintered by SPS, particles of a Ti-C-3Cu HEBM mixture with a shape close to spherical melted at the contacts [51]. It was shown that the contributions of a passing electric current (energy input by electric current) and the enthalpy of a chemical reaction to the structure formation of a material formed by reactive SPS can be "separated" [38]. This is done via conducting annealing/TE experiments outside the SPS chamber. In [38], the melting effect was not due to the heat of reaction but due to the passage of electric current through the contacts of small size. Figure 11 shows the microstructure of composites obtained from a Ti-C (carbon black)-3Cu non-milled powder mixture and a HEBM mixture of the same composition. The HEBM mixture consisted of nearly equiaxed composite particles. It is seen that the compact produced from the non-milled mixture contains agglomerates of TiC (dark regions in the image of Figure 11a). The microstructure of the composite sintered from the HEBM mixture is quite different: the copper matrix melts locally (bright regions), namely, at the inter-particle contacts (Figure 11b), while TiC particles are of the submicron size and do not form agglomerates [38].

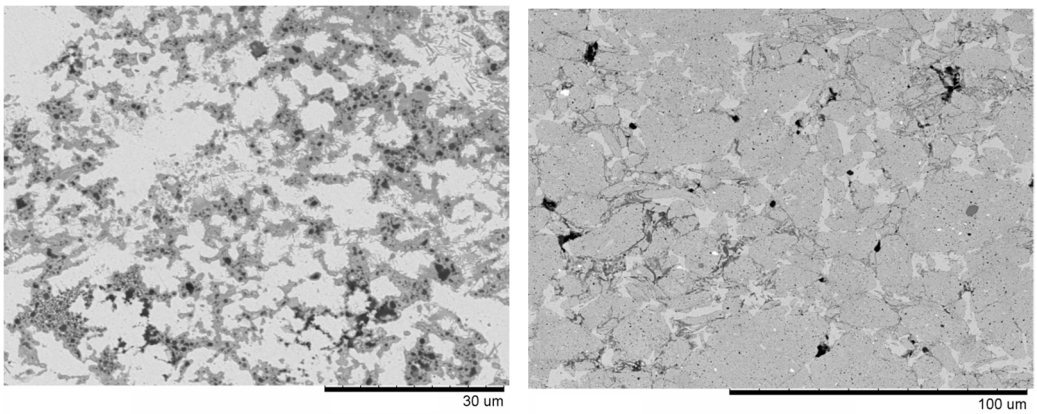

Figure 11. Microstructure (BSE images) of TiC-Cu composites formed by spark plasma sintering (SPS) of a non-milled Ti-C-3Cu mixture (**a**), a mixture subjected to HEBM for 10 min (**b**). Reprinted from [38], Copyright (2021), with permission from Elsevier.

Bulk materials obtained by SPS of HEBM composite powders can be used as precursors in the fabrication of porous materials [52–56]. In this case, one of the phases in the composite is sacrificial, which means that it is removed (selectively dissolved) to leave behind a porous skeleton made of the target phase. This method was applied to several systems: Fe-Ag [52,53], Ni-C [54] and Co-C [55]. In refs. [52,53], iron was selectively dissolved to form porous silver. Figure 12a shows the microstructure of a Fe-Ag pseudo-alloy produced by HEBM of the power obtained by wire electric explosion [53]. Upon the dissolution of iron, porous silver structures were formed (Figure 12b).

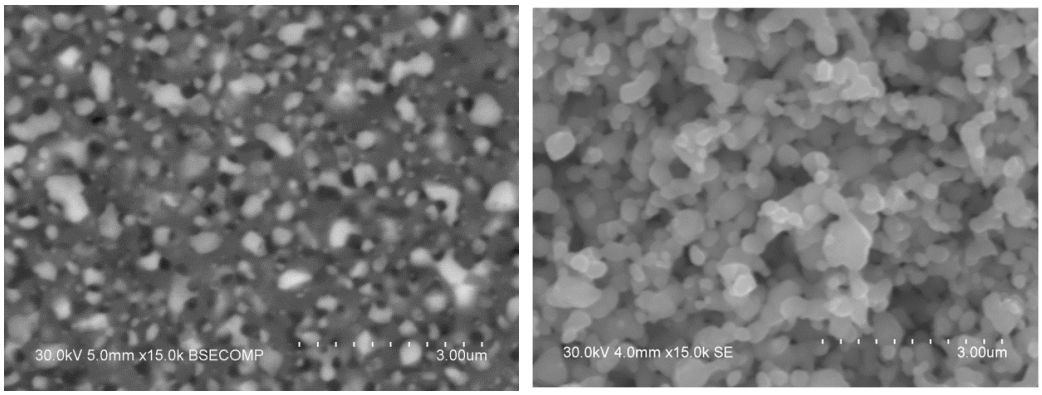

(**a**) (**b**)

Figure 12. Microstructure (BSE image) of the Fe-Ag pseudo-alloy obtained by SPS of the HEBM powder (**a**), morphology (SE image) of porous silver obtained by selective dissolution of iron from the sintered Fe-Ag pseudo-alloy (**b**). Reprinted from [53], Copyright (2022), with permission from Elsevier.

In the case of Ni-C and Co-C systems, mixtures of the metal and carbon black were subjected to HEBM. During SPS, nickel [54] or cobalt [55] served as a graphitization catalyst and a space holder. The metals were selectively dissolved from the sintered composites to form a porous graphitic material. The graphitization degree was higher in the compact sintered from the HEBM mixture than in the compact sintered from the non-milled mixture [54]. When iron was used to catalyze graphitization, the process was complicated by the formation of the Fe_3C phase, which was formed in the sintered materials [56].

2.3. Formation of Coatings from HEBM Powders

A series of studies conducted by our group were focused on the formation mechanisms, microstructure and properties of coatings obtained from HEBM powders by cold spraying (CS) [57–59] and detonation spraying (DS) [57,60–68]. The purpose of HEBM was to produce composite particles suitable for spraying or to form an alloy from the starting metallic components. In ref. [67], the possibility of obtaining alloy/composite coatings by DS of the Fe + Co + Ni and Fe + Co + Ni + Cu powder mixtures was evaluated. As exemplified in Figure 13, the deposited layers had a dense composite structure consisting of the metallic lamellae. Although the metal particles melted during the process, the alloying in the deposited layer was incomplete: the lamellae of the mixture components are clearly seen in the microstructure. Such coatings require an additional (post-spray) treatment by thermal annealing or laser irradiation. Insufficient alloying is not the only problem of the deposition of coatings from the powder blends. In refs. [67,69], partial loss of iron was observed during DS, which shifted the composition of the coatings toward Fe-depleted alloys. Recent studies on other systems show that the composition of the coating deposited by thermal spraying can be different from that of the feedstock powder mixture [70,71]. When a mixture of a Fe-based alloy and an alumina powder was subjected to DS, the losses of alumina were significant such that only a small fraction of alumina introduced into the powder mixture was found in the coatings [70]. This happens because of the large differences in the physical properties of the two powders. In the CS W-Cu coatings obtained from mixtures of the corresponding powders, the concentration of tungsten was lower than in the starting mixtures [71].

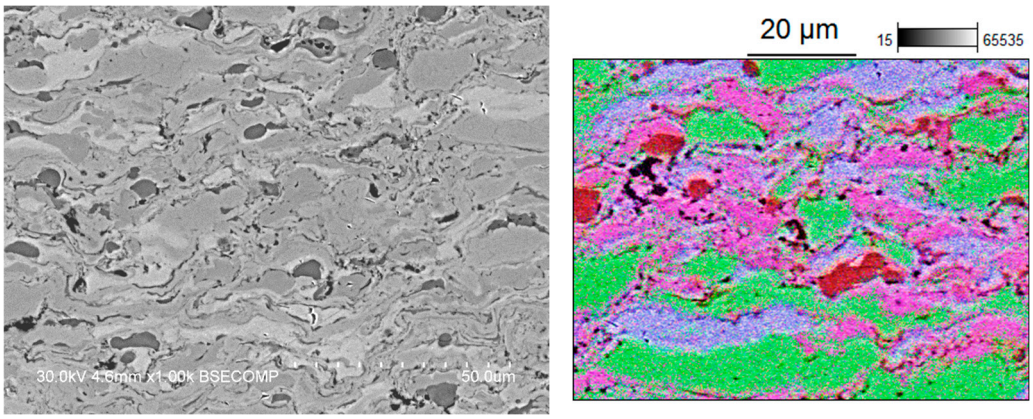

(**a**) (**b**)

Figure 13. Microstructure (BSE image) of the Fe-Co-Ni-Cu detonation coating (**a**), maps of the elements overlapping an image (**b**). Color in (**b**): red—Fe, purple—Co, green—Ni, blue—Cu. Reprinted from [67], Copyright (2021), with permission from Elsevier.

Another possibility to form a multi-component alloy coating is to use pre-alloyed powders. The formation of composite particles in the preparation of the feedstock powders for thermal spraying is critical for obtaining coatings with desired compositions. In our work, a FeCoNiCu alloy was obtained by HEBM (20 min) and deposited by DS [68]. The main phase of the DS coatings was a face-centered cubic solution. Coatings that were obtained using this approach do not require a post-spray treatment, as alloying was nearly complete after HEBM/DS.

2.4. The Role of HEBM in the Microstructure and Phase Formation of the Powder and Bulk Products

In Table 1, selected examples of materials obtained by our group (including those obtained in collaboration with other research laboratories) in the past two decades using HEBM are listed. In each case, the role of HEBM in the materials structure formation is given. When reaction mixtures are treated, HEBM allows lowering the combustion temperatures and switching to the solid-state interaction (combustion) mode. The reactivity of metals and intermetallics can be increased by preliminary HEBM. For some systems, it is impossible to obtain a single-phase product when conducting the synthesis in conventional (non-milled) mixtures. HEBM was shown to be instrumental in obtaining metastable states that decompose into the products with interesting particle morphologies. For the coating deposition by thermal spray technologies, the role of HEBM is the formation of composite or alloy particles.

Table 1. Selected examples of ceramic, intermetallic, metallic alloy and composite products obtained from HEBM powders.

Powder Mixture Subjected to HEBM	Processing Method of HEBM Powders	Phase Composition of the Product	Product State/Features	Role of HEBM	Reference
Powder products					
Ni + Al	SHS	Ni_3Al	powder	implementation of solid state combustion, formation of a single-phase nanocrystalline product	[17]
Ti + Al	TE	Ti_3Al	powder	formation of a single-phase nanocrystalline product	[34]

Table 1. *Cont.*

Powder Mixture Subjected to HEBM	Processing Method of HEBM Powders	Phase Composition of the Product	Product State/Features	Role of HEBM	Reference
Ni + B	TE	Ni_3B	powder	formation of a single-phase product	[32]
Ti + C + Si	SHS	Ti_3SiC_2	powder	formation of a single-phase product	[22]
Ti + Al + C	SHS	Ti_3AlC_2	powder	formation of a single-phase product	[22]
Fe−C	annealing	Fe(Fe_3C)@C	powder: core-shell particles	formation of non-equilibrium structures decomposing to form a graphitic shell	[40]
Ni−C	annealing	Ni@C	powder: core-shell particles	formation of non-equilibrium structures decomposing to form a graphitic shell	[40]
Mo + C	annealing	Mo_2C@C	powder: core-shell particles	formation of non-equilibrium structures decomposing to form a graphitic shell	[41]
Zr + C	annealing	ZrC@C	powder: core-shell particles	formation of non-equilibrium structures decomposing to form a graphitic shell	[42]
Hf + C	annealing	HfC@C	powder: core-shell particles	formation of non-equilibrium structures decomposing to form a graphitic shell	[42]
Fe + BN	annealing	Fe_2B@BN	powder: core-shell particles	formation of non-equilibrium structures decomposing to form a BN shell	[43]
Al + Cu + Fe	SHS	quasicrystalline phase	powder	formation of a single-phase product	[21]
Al + Ni + Co	SHS	quasicrystalline phase	powder	enabled SHS, formation of a single-phase product	[20]
Ti + BN	SHS	TiB_2-TiN	powder	formation of a nanocrystalline composite ceramic powder	[24]
Ti + B_4C	SHS	TiC-TiB_2	powder	formation of a submicron composite ceramic powder	[25]
Bulk alloys, ceramics, and composites					
Ti + C + Cu	reactive SPS	TiC−Cu	bulk composite	formation of a fine-grained composite, particle morphology control	[38,39,51]
Ti + B + Cu	SHS, SPS	TiB_2−Cu	bulk composite	formation of a fine-grained composite	[26,27,30]
Cu + Al	SPS	Cu(Al)	bulk alloy	alloy formation	[72]
Ni + C	SPS	Ni-graphite	bulk composite	mixing, structural refinement	[54]
Co + C	SPS	Co-graphite	bulk composite	mixing, structural refinement	[55]
Ni + W	SPS	Ni(W)-Ni_2W_4C-WC	bulk composite	alloy formation	[73,74]
Fe + Ag	SPS	Fe−Ag	bulk pseudo-alloy	structural refinement	[52,53]

Table 1. *Cont.*

Powder Mixture Subjected to HEBM	Processing Method of HEBM Powders	Phase Composition of the Product	Product State/Features	Role of HEBM	Reference
Ni + B	TE	Ni_3B	powder	formation of a single-phase product	[32]
Ni + Al + B	SPS	Ni_3Al−Ni(Al) alloyed with B	bulk composite	alloying with a minor additive	[75]
$Ti_{25}Cu_{75}$ + C	SPS	TiC−Cu	bulk composite	grinding of the alloy particles and mixing	[76,77]
Ti_3SiC_2 + Cu	SPS	Ti_3SiC_2−Cu. TiCx−Cu(Si)	bulk composite	mixing, particle morphology variation	[78]
Ti + B + Cu	shock consolidation	TiB_2-Cu	bulk composite	reaction completeness during consolidation	[79]
Ti + B + Cu	SHS, shock consolidation	TiB_2−Cu	bulk composite	formation of a fine-grained composite	[29]
		Coatings			
Fe + Co + Ni + Cu	DS	FeCoNiCu	coating, fcc alloy structure	alloy formation	[67]
Ti_3SiC_2 + Cu	DS	Ti_3SC_2−Cu, TiC_x-Cu(Si)	coating	formation of composite particles	[64,65]
Ti + C	TE, DS	Ti-titanium carbide (carbonitride)	coating	mixing, formation of composite particles	[62]
Ti + Al	TE, DS	titanium aluminides-titanium oxynitrides	coating	formation of a single-phase feedstock powder	[61,63]
Ti + B + Cu	SHS, DS	TiB_2−Cu	coating	formation of composite particles and a fine-grained composite	[57]
Ti + B + Cu	SHS, CS	TiB_2−Cu	coating	formation of composite particles and a fine-grained composite	[57,58]

3. Emerging Applications of HEBM Powders and Future Research Directions

The emerging applications of HEBM powders are in additive manufacturing. Recently, a successful application of HEBM powders as feedstock materials in laser-assisted additive manufacturing has been reported. Porous and dense materials were obtained by laser powder bed fusion of a Ti-Nb alloy produced by HEBM [80]. The powder particles were composed of nano-sized grains (up to 90 nm). The key requirement to the feedstock powder for additive manufacturing is the spherical (or close to spherical) shape of the particles. Ti-Nb particles formed by HEBM of the mixture of the metals were elliptical agglomerates and were suitable as the feedstock for the laser powder bed fusion technology. HEBM was, therefore, considered a promising alternative to spheroidization by plasma treatment or gas atomization. In ref. [81], a new approach was proposed: to use the heat of a chemical reaction to add to the laser power. A mixture of Ti and Al powders was subjected to HEBM to produce composite particles. The reaction-assisted production of Ti-Al intermetallics via selective laser melting was realized. It was noted that the onset temperature of the exothermic reaction was as low as 640 °C after HEBM. The described approach allows producing dense intermetallic and does not require the use of high-power lasers.

In future research, the applicability of HEBM powders as feedstock materials in additive manufacturing is to be elaborated for other systems, as the application potential exists for a broad range of compositions. More work is needed in the area of the formation of high-entropy and multi-component alloys by mechanical milling. Methods to control the distribution of minor additives in the milled metallic products should also be developed.

The scalability issue of HEBM should be addressed when transforming the method into a powder production technology. Although significant progress has been achieved in the development of materials using HEBM, further research is still needed. Both physical and chemical properties of fine-grained materials depend on their characteristic particle size [82]. Therefore, the control over the internal structure of the particles formed by HEBM of reaction mixtures is important for the outcome of the subsequent synthesis. The particle shape and size affect the results of sintering and thermal spraying. In this connection, studies aimed at finding ways to independently change the internal structure and morphology of the particles during milling would further advance the available technologies. Furthermore, in future research, a comparative analysis of the reactive sintering (including field-assisted sintering) and TE behavior of HEBM mixtures of different compositions should be performed. The structural development of materials upon initiation of TE by single pulses of electric current from a capacitor bank is also of scientific and practical interest.

4. Summary

HEBM is a useful method of powder treatment, which can be used in the processing of ceramics, intermetallics, alloys, and composite materials. The role of HEBM in the structure formation of the powder and bulk materials is manifold. HEBM can cause structural refinement, mixing of the reactants at the nanoscale, changes in the sintering behavior of powders, and the formation of alloy and composite particles suitable for further processing by high-energy fluxes. There are two ways to benefit from the formation of non-equilibrium structures by HEBM. One possibility is to preserve them in a bulk material or a coating to produce materials with enhanced properties. The other possibility is to use the relaxation of the non-equilibrium structures to advantage to produce materials with unusual particle morphologies. The synthesis routes of a variety of materials (intermetallics, alloys, ceramics, and composites) both in the powder and consolidated state were developed with the use of HEBM. Composite powders with a peculiar behavior under SPS conditions were obtained; the specifics of the sintering process were melting of the material at the inter-particle contacts and filling of the pores by the melt. In future research, the applicability of HEBM powders for additive manufacturing is to be elaborated for a broad range of systems, including multi-phase materials.

Author Contributions: Conceptualization, D.V.D. and B.B.B.; writing—original draft preparation, D.V.D.; writing—review and editing, B.B.B.; supervision, B.B.B.; funding acquisition, D.V.D. All authors have read and agreed to the published version of the manuscript.

Funding: This work was supported by the Ministry of Science and Higher Education of the Russian Federation (state assignment program), projects #121032500062-4 and #1021101115342-6.

Conflicts of Interest: The author declares no conflict of interest. The funders had no role in the design of the study; in the collection, analyses, or interpretation of data; in the writing of the manuscript, or in the decision to publish the results.

References

1. Zhang, D.L. Processing of advanced materials using high-energy mechanical milling. *Prog. Mater. Sci.* **2004**, *49*, 537–560. [CrossRef]
2. Boldyrev, V.V. Mechanochemistry and mechanical activation of solids. *Rus. Chem. Rev.* **2006**, *75*, 177–189. [CrossRef]
3. Baláž, P. High-energy milling. In *Mechanochemistry in Nanoscience and Minerals Engineering*; Springer: Berlin/Heidelberg, Germany, 2008; pp. 103–132.

4. Pentimalli, M.; Bellusci, M.; Padella, F. High-energy ball milling as a general tool for nanomaterials synthesis and processing. In *Handbook of Mechanical Nanostructuring*, 1st ed.; Aliofkhazraei, M., Ed.; Wiley-VCH Verlag GmbH & Co. KGaA: Weinheim, Germany, 2015; pp. 663–679.
5. El-Eskandarany, M.S.; Al-Hazza, A.; Al-Hajji, L.A.; Ali, N.; Al-Duweesh, A.A.; Banyan, M.; Al-Ajmi, F. Mechanical milling: A superior nanotechnological tool for fabrication of nanocrystalline and nanocomposite materials. *Nanomaterials* **2021**, *11*, 2484. [CrossRef]
6. Lapshin, O.V.; Smolyakov, V.K. Modeling the synthesis of mechanocomposites in binary systems. *Comb. Explos. Shock Waves* **2011**, *47*, 553–562. [CrossRef]
7. Lapshin, O.V.; Ryabkova, A.I. Mathematical model of the formation of mechanocomposite particles during the mechanical treatment of a powder mixture. *J. Phys. Conf. Ser.* **2019**, *1214*, 012013. [CrossRef]
8. Suryanarayana, C.; Al-Aqeeli, N. Mechanically alloyed nanocomposites. *Prog. Mater. Sci.* **2013**, *58*, 383–502. [CrossRef]
9. Hadef, F. Synthesis and disordering of B2 TM-Al (TM = Fe, Ni, Co) intermetallic alloys by high energy ball milling: A review. *Powder Technol.* **2017**, *311*, 556–578. [CrossRef]
10. Rogachev, A.S. Mechanical activation of heterogeneous exothermic reactions in powder mixtures. *Russ. Chem. Rev.* **2019**, *88*, 875–900. [CrossRef]
11. Burmeister, C.F.; Kwade, A. Process engineering with planetary ball mills. *Chem. Soc. Rev.* **2013**, *42*, 7660–7667. [CrossRef]
12. Avvakumov, E.G.; Potkin, A.R.; Samarin, O.I. A planetary mill. *USSR Invent. Bull.* **1982**, *43*, 975068.
13. Kwon, Y.S.; Gerasimov, K.B.; Yoon, S.K. Ball temperatures during mechanical alloying in planetary mills. *J. Alloys Compd.* **2002**, *346*, 276–281. [CrossRef]
14. Rogachev, A.S.; Mukasyan, A.S. *Combustion for Material Synthesis*; CRC Press: London, UK, 2014; 424p.
15. Mukasyan, A.S.; Rogachev, A.S.; ThippaReddy Aruna, S. Combustion synthesis in nanostructured reactive systems. *Adv. Powder Technol.* **2015**, *26*, 954–976. [CrossRef]
16. Vidyuk, T.M.; Korchagin, M.A.; Dudina, D.V.; Bokhonov, B.B. Synthesis of ceramic and composite materials using a combination of self-propagating high-temperature synthesis and spark plasma sintering (Review). *Comb. Explos. Shock Waves* **2021**, *57*, 385–397. [CrossRef]
17. Korchagin, M.A.; Grigor'eva, T.F.; Bokhonov, B.B.; Sharafutdinov, M.R.; Barinova, A.P.; Lyakhov, N. Solid-state combustion in mechanically activated SHS systems. I. Effect of activation time on process parameters and combustion product composition. *Comb. Explos. Shock Waves* **2003**, *39*, 43–50. [CrossRef]
18. Korchagin, M.A.; Grigor'eva, T.F.; Bokhonov, B.B.; Sharafutdinov, M.R.; Barinova, A.P.; Lyakhov, N. Solid-state combustion in mechanically activated SHS systems. II. Effect of mechanical activation conditions on process parameters and combustion product composition. *Comb. Explos. Shock Waves* **2003**, *39*, 51–58. [CrossRef]
19. Ditenberg, I.A.; Osipov, D.A.; Korchagin, M.A.; Smirnov, I.V.; Grinyaev, K.V.; Gavrilov, A.I. Influence of ball milling duration on the morphology, features of the structural-phase state and microhardness of 3Ni-Al powder mixture. *Adv. Powder Technol.* **2021**, *32*, 3447–3455. [CrossRef]
20. Korchagin, M.A.; Bokhonov, B.B. Self-propagating high-temperature synthesis of quasicrystals. *Comb. Explos. Shock Waves* **2004**, *40*, 438–444. [CrossRef]
21. Bokhonov, B.B. Mechanical alloying and self-propagating high-temperature synthesis of stable icosahedral quasicrystals. *J. Alloys Compd.* **2008**, *461*, 150–153. [CrossRef]
22. Korchagin, M.A.; Gavrilov, A.I.; Grishina, I.V.; Dudina, D.V.; Ukhina, A.V.; Bokhonov, B.B.; Lyakhov, N.Z. Self-propagating high-temperature synthesis of Ti_3SiC_2 and Ti_3AlC_2 single-phase MAX phases in mechanically activated mixtures of initial reactants. *Comb. Explos. Shock Waves* **2022**, *58*, 46–53. [CrossRef]
23. Korchagin, M.A.; Gavrilov, A.I.; Dudina, D.V.; Bokhonov, B.B.; Bulina, N.V. Hedvall effect in self-propagating high-temperature synthesis in mechanically activated compositions. *Comb. Explos. Shock Waves* **2021**, *57*, 640–650. [CrossRef]
24. Korchagin, M.A.; Bokhonov, B.B. Combustion of mechanically activated 3Ti+2BN mixtures. *Comb. Explos. Shock Waves* **2010**, *46*, 170–177. [CrossRef]
25. Korchagin, M.A.; Gavrilov, A.I.; Zarko, V.E.; Kiskin, A.B.; Iordan, Y.V.; Trushlyakov, V.I. Self-propagating high-temperature synthesis in mechanically activated mixtures of boron carbide and titanium. *Comb. Explos. Shock Waves* **2017**, *53*, 669–677. [CrossRef]
26. Kwon, Y.S.; Dudina, D.V.; Korchagin, M.A.; Lomovsky, O.I. Microstructure changes in TiB_2-Cu nanocomposite under sintering. *J. Mater. Sci.* **2004**, *39*, 5325–5331. [CrossRef]
27. Kim, J.S.; Kwon, Y.-S.; Lomovsky, O.I.; Korchagin, M.; Mali, V.; Dudina, D. A synthetic route for metal-ceramic interpenetrating phase composites. *Mater. Lett.* **2006**, *60*, 3723–3726. [CrossRef]
28. Korchagin, M.A.; Dudina, D.V. Application of self-propagating high-temperature synthesis and mechanical activation for obtaining nanocomposites. *Comb. Explos. Shock Waves* **2007**, *43*, 176–187. [CrossRef]
29. Kim, J.S.; Kwon, Y.S.; Dudina, D.V.; Lomovsky, O.I.; Korchagin, M.A.; Mali, V.I. Nanocomposites TiB_2-Cu: Consolidation and erosion behavior. *J. Mater. Sci.* **2005**, *40*, 3491–3495. [CrossRef]
30. Kim, J.S.; Dudina, D.V.; Kim, J.C.; Kwon, Y.S.; Park, J.J.; Rhee, C.K. Properties of Cu-based nanocomposites produced by mechanically activated self-propagating high-temperature synthesis and spark-plasma sintering. *J. Nanosci. Nanotechnol.* **2010**, *10*, 252–257. [CrossRef]

31. Korchagin, M.A.; Gabdrashova, S.E.; Dudina, D.V.; Bokhonov, B.B.; Bulina, N.V.; Kuznetsov, V.L.; Ishchenko, A.V. Combustion characteristics and structure of carbon nanotube/titanium composites. *J. Thermal Anal. Calorim.* **2019**, *137*, 1903–1910. [CrossRef]
32. Korchagin, M.A.; Dudina, D.V.; Bokhonov, B.B.; Bulina, N.V.; Ukhina, A.V.; Batraev, I.S. Synthesis of nickel boride by thermal explosion in ball-milled powder mixtures. *J. Mater. Sci.* **2018**, *53*, 13592–13599. [CrossRef]
33. Korchagin, M.A.; Bulina, N.V. Superadiabatic regime of the thermal explosion in a mechanically activated mixture of tungsten with carbon black. *Comb. Explos. Shock Waves* **2016**, *52*, 225–233. [CrossRef]
34. Filimonov, V.Y.; Korchagin, M.A.; Dietenberg, I.A.; Tyumentsev, A.N.; Lyakhov, N.Z. High temperature synthesis of single-phase Ti_3Al intermetallic compound in mechanically activated powder mixture. *Powder Technol.* **2013**, *235*, 606–613. [CrossRef]
35. Korchagin, M.A. Thermal explosion in mechanically activated low-calorific-value compositions. *Comb. Explos. Shock Waves* **2015**, *51*, 578–586. [CrossRef]
36. Korchagin, M.A.; Avvakumov, E.G.; Lepezin, G.G.; Vinokurova, O.B. Thermal explosion and self-propagating high-temperature synthesis in mechanically activated SiO_2-Al mixtures. *Comb. Explos. Shock Waves* **2014**, *50*, 641–646. [CrossRef]
37. Filimonov, V.Y.; Korchagin, M.A.; Smirnov, E.V.; Lyakhov, N.Z. Macrokinetics of solid-phase synthesis of an activated 3Ni + Al mixture in the thermal explosion mode. *Comb. Explos. Shock Waves* **2010**, *46*, 449–456. [CrossRef]
38. Dudina, D.V.; Vidyuk, T.M.; Gavrilov, A.I.; Ukhina, A.V.; Bokhonov, B.B.; Legan, M.A.; Matvienko, A.A.; Korchagin, M.A. Separating the reaction and spark plasma sintering effects during the formation of TiC–Cu composites from mechanically milled Ti–C–3Cu mixtures. *Ceram. Int.* **2021**, *47*, 12494–12504. [CrossRef]
39. Vidyuk, T.M.; Dudina, D.V.; Korchagin, M.A.; Gavrilov, A.I.; Ukhina, A.V.; Bulanova, U.E.; Legan, M.A.; Novoselov, A.N.; Esikov, M.A.; Anisimov, A.G. Manufacturing of TiC-Cu composites by mechanical milling and spark plasma sintering using different carbon sources. *Surf. Interf.* **2021**, *27*, 101445. [CrossRef]
40. Bokhonov, B.; Korchagin, M. The formation of graphite encapsulated metal nanoparticles during mechanical activation and annealing of soot with iron and nickel. *J. Alloys Compd.* **2002**, *333*, 308–320. [CrossRef]
41. Bokhonov, B.; Borisova, Y.; Korchagin, M. Formation of encapsulated molybdenum carbide particles by annealing mechanically activated mixtures of amorphous carbon with molybdenum. *Carbon* **2004**, *42*, 2067–2071. [CrossRef]
42. Bokhonov, B.B.; Dudina, D.V. Synthesis of ZrC and HfC nanoparticles encapsulated in graphitic shells from mechanically milled Zr-C and Hf-C powder mixtures. *Ceram. Int.* **2017**, *43*, 14529–14532. [CrossRef]
43. Bokhonov, B.; Korchagin, M.; Borisova, Y. Formation of nanosized particles encapsulated in boron nitride during low-temperature annealing of mechanochemically treated Fe–BN mixtures. *J. Alloys Compd.* **2004**, *372*, 141–147. [CrossRef]
44. Dudina, D.V.; Mukherjee, A.K. Reactive Spark Plasma Sintering: Successes and challenges of nanomaterial synthesis. *J. Nanomater.* **2013**, *2013*, 625218. [CrossRef]
45. Orrù, R.; Licheri, R.; Locci, A.M.; Cao, G. Mechanochemically activated powders as precursors for spark plasma sintering (SPS) processes. In *High-Energy Ball Milling: Mechanochemical Processing of Nanopowders*; Sopicka-Lizer, M., Ed.; Woodhead Publishing: Sawston, UK, 2010; pp. 275–303.
46. Olevsky, E.A.; Dudina, D.V. *Field-Assisted Sintering: Science and Applications*; Springer International Publishing: Cham, Switzerland, 2018; 425p.
47. Mukasyan, A.S.; Rogachev, A.S.; Moskovskikh, D.O.; Yermekova, Z.S. Reactive spark plasma sintering of exothermic systems: A critical review. *Ceram. Int.* **2022**, *48*, 2988–2998. [CrossRef]
48. Dudina, D.V.; Vidyuk, T.M.; Korchagin, M.A. Synthesis of ceramic reinforcements in metallic matrices during spark plasma sintering: Consideration of reactant/matrix mutual chemistry. *Ceramics* **2021**, *4*, 592–599. [CrossRef]
49. Cabouro, G.; Chevalier, S.; Gaffet, E.; Grin, Y.; Bernard, F. Reactive sintering of molybdenum disilicide by spark plasma sintering from mechanically activated powder mixtures: Processing parameters and properties. *J. Alloys Compd.* **2008**, *465*, 344–355. [CrossRef]
50. Paris, S.; Gaffet, E.; Bernard, F.; Munir, Z.A. Spark plasma synthesis from mechanically activated powders: A versatile route for producing dense nanostructured iron aluminides. *Scr. Mater.* **2004**, *50*, 691–696. [CrossRef]
51. Vidyuk, T.M.; Dudina, D.V.; Korchagin, M.A.; Gavrilov, A.I.; Skripkina, T.S.; Ukhina, A.V.; Anisimov, A.G.; Bokhonov, B.B. Melting at the inter-particle contacts during Spark Plasma Sintering: Direct microstructural evidence and relation to particle morphology. *Vacuum* **2020**, *181*, 109566. [CrossRef]
52. Bokhonov, B.B.; Dudina, D.V. Recrystallisation-accompanied phase separation in Ag–Fe and Ag–Ni nanocomposites: A route to structure tailoring of nanoporous silver. *RSC Adv.* **2013**, *3*, 12655. [CrossRef]
53. Petrov, S.A.; Bokhonov, B.B.; Dudina, D.V.; Korchagin, M.A.; Gavrilov, A.I.; Ukhina, A.V.; Bakina, O.V.; Lerner, M.I. Fe-Ag pseudo-alloys obtained by wire electric explosion, ball milling and spark plasma sintering. *Mater. Lett.* **2022**, *323*, 132536. [CrossRef]
54. Bokhonov, B.B.; Dudina, D.V.; Ukhina, A.V.; Korchagin, M.A.; Bulina, N.V.; Mali, V.I.; Anisimov, A.G. Formation of self-supporting porous graphite structures by Spark Plasma Sintering of nickel-amorphous carbon mixtures. *J. Phys. Chem. Solids* **2015**, *76*, 192–202. [CrossRef]
55. Bokhonov, B.B.; Korchagin, M.A.; Ukhina, A.V.; Dudina, D.V. Structural and morphological transformations in cobalt-carbon mixtures during ball milling, annealing and Spark Plasma Sintering. *Vacuum* **2018**, *157*, 210–215. [CrossRef]

56. Dudina, D.V.; Ukhina, A.V.; Bokhonov, B.B.; Korchagin, M.A.; Bulina, N.V.; Kato, H. The influence of the formation of Fe_3C on graphitization in a carbon-rich iron-amorphous carbon mixture processed by Spark Plasma Sintering and annealing. *Ceram. Int.* **2017**, *43*, 11902–11906. [CrossRef]
57. Lomovsky, O.I.; Dudina, D.V.; Ulianitsky, V.Y.; Zlobin, S.; Kosarev, V.; Klinkov, S.; Korchagin, M.; Kwon, D.H.; Kim, J.S.; Kwon, Y.S. Cold and detonation spraying of TiB_2-Cu nanocomposites. *Mater. Sci. Forum* **2007**, *534*, 1373–1376. [CrossRef]
58. Kim, J.S.; Kwon, Y.S.; Lomovsky, O.I.; Dudina, D.; Kosarev, V.; Klinkov, S.; Kwon, D.; Smurov, I. Cold spraying of in situ produced TiB_2-Cu nanocomposite powders. *Comp. Sci. Technol.* **2007**, *67*, 2292–2296. [CrossRef]
59. Vidyuk, T.M.; Dudina, D.V.; Korchagin, M.A.; Gavrilov, A.I.; Bokhonov, B.B.; Ukhina, A.V.; Esikov, M.A.; Shikalov, S.V.; Kosarev, V.F. Spark plasma sintering treatment of cold sprayed materials for synthesis and structural modification: A case study using TiC-Cu composites. *Mater. Lett. X* **2022**, *14*, 100140. [CrossRef]
60. Dudina, D.V.; Batraev, I.S.; Ulianitsky, V.Y.; Korchagin, M.A. Possibilities of the computer-controlled detonation spraying method: A chemistry viewpoint. *Ceram. Int.* **2014**, *40*, 3253–3260. [CrossRef]
61. Dudina, D.V.; Korchagin, M.A.; Zlobin, S.B.; Ulianitsky, V.Y.; Lomovsky, O.I.; Bulina, N.V.; Bataev, I.A.; Bataev, V.A. Compositional variations in the coatings formed by detonation spraying of Ti_3Al at different O_2/C_2H_2 ratios. *Intermetallics* **2012**, *29*, 140–146. [CrossRef]
62. Dudina, D.V.; Pribytkov, G.A.; Krinitcyn, M.G.; Korchagin, M.A.; Bulina, N.V.; Bokhonov, B.B.; Batraev, I.S.; Rybin, D.K.; Ulianitsky, V.Y. Detonation spraying behavior of TiC_x-Ti powders and the role of reactive processes in the coating formation. *Ceram. Int.* **2016**, *42*, 690–696. [CrossRef]
63. Dudina, D.V.; Batraev, I.S.; Ulianitsky, V.Y.; Bulina, N.V.; Korchagin, M.A.; Lomovsky, O. Detonation spraying of Ti–Al intermetallics: Phase and microstructure development of the coatings. *Mater. Manuf. Proc.* **2015**, *30*, 724–729. [CrossRef]
64. Dudina, D.V.; Batraev, I.S.; Ulianitsky, V.Y.; Bulina, N.V.; Korchagin, M.A.; Bataev, I.A.; Jorge, A.M. Formation routes of nanocomposite coatings in detonation spraying of Ti_3SiC_2-Cu powders. *J. Thermal Spray Technol.* **2014**, *23*, 1116–1123. [CrossRef]
65. Dudina, D.V.; Batraev, I.S.; Ulianitsky, V.Y.; Korchagin, M.A.; Golubkova, G.V.; Abramov, S.Y.; Lomovsky, O. Control of interfacial interaction during detonation spraying of Ti_3SiC_2–Cu composites. *Inorg. Mater.* **2014**, *50*, 35–39. [CrossRef]
66. Ulianitsky, V.Y.; Dudina, D.V.; Shtertser, A.A.; Smurov, I. Computer-controlled detonation spraying: Flexible control of the coating chemistry and microstructure. *Metals* **2019**, *9*, 1244. [CrossRef]
67. Ulianitsky, V.Y.; Rybin, D.K.; Ukhina, A.V.; Bokhonov, B.B.; Dudina, D.V.; Samodurova, M.N.; Trofimov, E.A. Structure and composition of Fe-Co-Ni and Fe-Co-Ni-Cu coatings obtained by detonation spraying of powder mixtures. *Mater. Lett.* **2021**, *290*, 129498. [CrossRef]
68. Ulianitsky, V.Y.; Korchagin, M.A.; Gavrilov, A.I.; Batraev, I.S.; Rybin, D.K.; Ukhina, A.V.; Dudina, D.V.; Samodurova, M.N.; Trofimov, E.A. FeCoNiCu alloys obtained by detonation spraying and spark plasma sintering of high-energy ball-milled powders. *J. Therm. Spray Technol.* **2022**, *31*, 1067–1075. [CrossRef]
69. Ulianitsky, V.Y.; Rybin, D.K.; Sova, A.; Moghaddam, A.O.; Samodurova, M.; Doubenskaia, M.; Trofimov, E. Formation of metal composites by detonation spray of powder mixtures. *Int. J. Adv. Manuf. Technol.* **2021**, *117*, 81–95. [CrossRef]
70. Kuchumova, I.D.; Cherkasova, N.Y.; Batraev, I.S.; Shikalov, V.S.; Ukhina, A.V.; Koga, G.Y.; Jorge, A.M. Wear-resistant Fe-based metallic glass-Al_2O_3 composite coatings produced by detonation spraying. *J. Therm. Spray Technol.* **2022**, *31*, 1355–1365. [CrossRef]
71. Shikalov, V.S.; Vidyuk, T.M.; Filippov, A.A.; Kuchumova, I.D. Microstructure, mechanical and tribological properties of cold sprayed Cu–W coatings. *Int. J. Refract. Metals Hard Mater.* **2022**, *106*, 105866. [CrossRef]
72. Dudina, D.V.; Grigoreva, T.F.; Kvashnin, V.I.; Devyatkina, E.T.; Vosmerikov, S.V.; Ukhina, A.V.; Novoselov, A.N.; Legan, M.A.; Esikov, M.A.; Lukyanov, Y.L.; et al. Microstructure and properties of Cu-10 wt% Al bronze obtained by high-energy mechanical milling and spark plasma sintering. *Mater. Lett.* **2022**, *312*, 131671. [CrossRef]
73. Bokhonov, B.B.; Ukhina, A.V.; Dudina, D.V.; Anisimov, A.G.; Mali, V.I.; Batraev, I.S. Carbon uptake during Spark Plasma Sintering: Investigation through the analysis of the carbide "footprint" in a Ni–W alloy. *RSC Adv.* **2015**, *5*, 80228–80237. [CrossRef]
74. Dudina, D.V.; Bokhonov, B.B.; Ukhina, A.V.; Anisimov, A.G.; Mali, V.I.; Esikov, M.A.; Batraev, I.S.; Kuznechik, O.O.; Pilinevich, L.P. Reactivity of materials towards carbon of graphite foil during Spark Plasma Sintering: A case study using Ni–W powders. *Mater. Lett.* **2016**, *168*, 62–67. [CrossRef]
75. Shevtsova, L.I.; Korchagin, M.A.; Esikov, M.A.; Lozhkina, E.; Lozhkin, V.; Samoylenko, V.; Nemolochnov, D.; Malicov, V. Ni_3Al+B material obtained by mechanical activation followed by spark plasma sintering. *Mater. Today Proc.* **2019**, *12*, 120–123. [CrossRef]
76. Dudina, D.V.; Vidyuk, T.M.; Korchagin, M.A.; Gavrilov, A.I.; Bulina, N.V.; Esikov, M.A.; Datekyu, M.; Kato, H. Interaction of a Ti–Cu alloy with carbon: Synthesis of composites and model experiments. *Materials* **2019**, *12*, 1482. [CrossRef] [PubMed]
77. Dudina, D.V.; Korchagin, M.A.; Gavrilov, A.I.; Bulina, N.V.; Batraev, I.S.; Esikov, M.A.; Batraev, I.S.; Esikov, M.A.; Georgarakis, K.; Kato, H. Formation of TiC-Cu nanocomposites by a reaction between $Ti_{25}Cu_{75}$ melt-spun alloy and carbon. *Mater. Lett.* **2019**, *235*, 104–106. [CrossRef]
78. Dudina, D.V.; Mali, V.I.; Anisimov, A.G.; Bulina, N.V.; Korchagin, M.A.; Lomovsky, O.I.; Bataev, I.A.; Bataev, V.A. Ti_3SiC_2-Cu composites by mechanical milling and Spark Plasma Sintering: Possible microstructure formation scenarios. *Metals Mater. Int.* **2013**, *19*, 1235–1241. [CrossRef]
79. Dudina, D.V.; Mali, V.I.; Anisimov, A.G.; Lomovsky, O.I. Shock compression of Ti–B–Cu powder mixtures: Microstructural aspects. *Mater. Sci. Eng. A* **2009**, *503*, 41–44. [CrossRef]

80. Khimich, M.A.; Prosolov, K.A.; Mishurova, T.; Evsevleev, S.; Monforte, X.; Teuschl, A.; Slezak, P.; Ibragimov, E.; Saprykin, A.; Kovalevskaya, Z.; et al. Advances in laser additive manufacturing of Ti-Nb alloys: From nanostructured powders to bulk objects. *Nanomaterials* **2021**, *11*, 1159. [CrossRef] [PubMed]
81. Nepapushev, A.A.; Moskovskikh, D.O.; Vorotilo, K.V.; Rogachev, A.S. TiAl-based materials by in situ selective laser melting of Ti/Al reactive composites. *Metals* **2020**, *10*, 1505. [CrossRef]
82. Shekhawat, D.; Vauth, M.; Pezoldt, J. Size dependent properties of reactive materials. *Inorganics* **2022**, *10*, 56. [CrossRef]